J. Fluid Mech. (2007), *vol.* 572, *pp.* 219–229. © 2007 Cambridge University Press
doi:10.1017/S0022112006003661 Printed in the United Kingdom

Fast scalar decay in a shear flow: modes and pseudomodes

By J. VANNESTE AND J. G. BYATT-SMITH

School of Mathematics, University of Edinburgh, King's Buildings, Edinburgh EH9 3JZ, UK

(Received 18 August 2006 and in revised form 10 October 2006)

The decay of a passive scalar in a sinusoidal shear flow translating in the cross-stream direction at a constant speed u is studied in the limit of small diffusivity κ. The decay rate, obtained by solving an eigenvalue problem, is found to tend to a non-zero constant as $\kappa \to 0$ when u is of order $\kappa^{1/2}$. This result, establishing that fast decay is possible in shear flows, is fragile however: because of the existence of pseudomodes, the addition of a small noise leads to decay rates that decrease to zero with κ as $\kappa^{2/5}$.

1. Introduction

The aim of this paper is to provide an example of a unidirectional flow in which the decay of a passive scalar is fast. By fast decay, we mean that the rate at which fluctuations of the scalar concentration decay in the long-time limit is independent of the diffusivity κ as this tends to zero (or, equivalently, independent of the Péclet number as this tends to infinity). Fast decay in this sense is known to occur in some two-dimensional random flows (see, e.g., Pierrehumbert 1994; Antonsen *et al.* 1996; Tsang, Antonsen & Ott 2005; Haynes & Vanneste 2005). A crucial ingredient of these flows, in addition to the spatial smoothness and bounded domain ensuring exponential decay, is that they are stretching: particle trajectories separate exponentially fast, leading to a rapid thinning of the scalar structures down to a diffusive scale proportional to $\kappa^{1/2}$. Here, by contrast, we consider a flow in which the particle separation is only linear in time.

The flow under study is a simple sinusoidal shear flow, translating in the cross-stream direction at a constant speed u. In the absence of translation, $u = 0$, the scalar decay rate decreases to 0 as $\kappa^{1/2}$ when $\kappa \to 0$ (Bajer, Bassom & Gilbert 2001; Gleeson *et al.* 2004; Giona, Cerbelli & Vitacolonna 2004). However, we show that if u is chosen suitably, specifically taken proportional to $\kappa^{1/2}$, the decay rate tends to a non-zero constant. We note that the effect of a translation $u \neq 0$, or rather, of the equivalent addition to a steady shear of a uniform cross-stream flow, has been studied in the context of homogenization (Childress & Soward 1990; Majda & McLaughlin 1993). The results of these studies are, however, not relevant to the long-time decay considered here, because this is controlled by scalar structures with scales much smaller than the flow scale.

The possibility of fast decay in translating shear flows suggests that they might be useful in mixing devices. There are, however, several caveats to keep in mind when comparing their efficiency to that of the stretching flows more typically considered for this purpose (Wiggins & Ottino 2004). First, the fast-decay property applies only to scalar concentration with vanishing average in the streamwise direction, since this average is unaffected by the flow. Second, the fast decay characterizes only the long-time behaviour of the scalar, and the time taken to reduce the concentration

https://doi.org/10.1017/S0022112006003661 Published online by Cambridge University Press

fluctuations by a fixed, order-one factor is much longer in shear flows, even with $u \neq 0$, than in stretching flows. Third, and this is a point which we discuss in some detail, the property of fast mixing is not a robust one. Specifically, although the long-time decay is in principle controlled by an eigenmode of the advection–diffusion operator, pseudomodes (i.e. approximate solutions of the eigenvalue problem with exponentially small errors) play a major transient role: in the presence of small noise (including round-off errors in numerical simulations), they control the decay rate, which we show scales like $\kappa^{2/5}$.

2. Formulation

We consider the decay of a passive scalar advected by the steadily translating shear flow

$$\boldsymbol{v} = (0, \alpha \sin(x - ut)), \tag{2.1}$$

where α and u are two positive constants. The domain is taken to be doubly periodic, and in the scaled spatial variables chosen for (2.1) is $(x, y) \in [0, 2\pi] \times [0, 2\pi L]$, where L is its aspect ratio. The concentration $C(x, y, t)$ of the passive scalar obeys the advection–diffusion equation

$$C_t + \alpha \sin(x - ut) C_y = \kappa (C_{xx} + C_{yy}),$$

where κ is the molecular diffusivity. Because this equation is independent of y, its solution can be expressed as a sum of independent Fourier modes. Concentrating on one such mode, we write

$$C(x, y, t) = \mathrm{Re}\, \hat{C}(x, t) \mathrm{e}^{\mathrm{i}ly - \kappa l^2 t},$$

where l is one of the wavenumbers n/L, with $n = 0, 1, 2, \cdots$, and obtain

$$\hat{C}_t + \mathrm{i}\alpha l \sin(x - ut) \hat{C} = \kappa \hat{C}_{xx}. \tag{2.2}$$

The y-independent mode $l = 0$ is unaffected by advection and decays purely diffusively; we ignore this mode in what follows, assuming that the initial concentration satisfies

$$\int_0^L C(x, y, 0)\, \mathrm{d}y = 0.$$

It is convenient to make (2.2) time independent by introducing the coordinate $x' = x - ut$, that is, by using a frame of reference translating with speed u in the x-direction. It is also convenient to non-dimensionalize t, u and κ by introducing $t' = \alpha l t$, $u' = u/(\alpha l)$ and $\kappa' = \kappa/(\alpha l)$. Omitting the primes, this transforms (2.2) into

$$\hat{C}_t - u \hat{C}_x + \mathrm{i} \sin x\, \hat{C} = \kappa \hat{C}_{xx}. \tag{2.3}$$

In this formulation, u is the ratio of the translation speed of the flow pattern (2.1) to the maximum flow speed, and κ is an inverse Péclet number.

3. Eigenvalue problem

We are interested in the long-time decay of the concentration. Clearly, this is controlled by the spectrum of the operator associated with (2.3). Specifically, we write

$$\hat{C}(x, t) = \theta(x) \exp(-\lambda t),$$

https://doi.org/10.1017/S0022112006003661 Published online by Cambridge University Press

to find the eigenvalue problem

$$-\kappa\theta_{xx} - u\theta_x + \mathrm{i}\sin x\,\theta = \lambda\theta, \quad \text{with } \theta(x+2\pi) = \theta(x). \tag{3.1}$$

The corresponding spectrum consists of a countable set of eigenvalues λ with positive real parts. The eigenvalue with the smallest real part, which we simply denote by λ, gives the decay rate of the concentration as $t \to \infty$. We now examine the dependence of this eigenvalue on κ and u in the large-Péclet-number limit $\kappa \to 0$.

We first note that when the shear is steady, that is, when $u = 0$, the decay rate is proportional to $\kappa^{1/2}$. Indeed, a simple boundary-layer analysis (extended below) gives

$$\mathrm{Re}\,\lambda \sim \frac{\kappa^{1/2}}{2} \quad \text{for } u = 0, \tag{3.2}$$

with the corresponding eigenfunction $\theta(x)$ localized near either of the extrema $x = \pi/2$ and $x = 3\pi/2$ of the velocity profile. The vanishing of the shear at these two points limits the efficiency of the mixing and leads to the $\kappa^{1/2}$ power law (Bajer *et al.* 2001; Giona *et al.* 2004). Intuitively, one might expect that a non-zero translation speed $u \neq 0$ makes the mixing more efficient by constantly shifting the position of the velocity extrema. This is not necessarily the case, however: a short computation shows that

$$\mathrm{Re}\,\lambda \sim \frac{\kappa}{2u^2} \quad \text{for } u = O(1). \tag{3.3}$$

This is asymptotically smaller than (3.2), so an $O(1)$ translation decreases the mixing efficiency. However, (3.3) indicates that $\mathrm{Re}\,\lambda$ increases as u decreases, leaving open the possibility that $\mathrm{Re}\,\lambda \gg \kappa^{1/2}$ for some asymptotically small but non-zero u. We examine this possibility by considering the case where $u = O(\kappa^{1/2})$. We therefore let

$$u = \kappa^{1/2} w \quad \text{with } w = O(1). \tag{3.4}$$

In this regime, the decay rate $\mathrm{Re}\,\lambda$ belongs to either of two eigenvalue branches, depending on w. The first branch continues (3.2) as u increases from 0 and can be approximated by a boundary-layer analysis; the second branch continues (3.3) as u decreases from $O(1)$ values and can approximated using a WKB expansion. We present these two approximations next.

3.1. *Boundary-layer analysis*

Motivated by the solution for $u = 0$, we seek a localized solution and introduce the expansions

$$\theta(x) = \mathrm{e}^{-wx/(2\kappa^{1/2})}\left[\Theta^{(0)}(X) + \kappa^{1/2}\Theta^{(1)}(X) + \cdots\right]$$

and $\lambda = w^2/4 + \mathrm{i} + \kappa^{1/2}\lambda^{(1)} + \cdots$, where $X = \kappa^{-1/4}(x - \pi/2)$ and the functions $\Theta^{(i)}(X)$ are assumed to be localized near $X = 0$. This gives the leading-order eigenvalue problem

$$\Theta'' + \left(\lambda^{(1)} + \mathrm{i}\frac{X^2}{2}\right)\Theta = 0.$$

The solution of interest, with smallest $\mathrm{Re}\,\lambda$, is simply given by the Gaussian

$$\Theta^{(0)}(X) = \mathrm{e}^{-(1-\mathrm{i})X^2/4}, \quad \text{with} \quad \lambda^{(1)} = (1-\mathrm{i})/2.$$

Hence we obtain the approximation

$$\mathrm{Re}\,\lambda = \frac{w^2}{4} + \frac{\kappa^{1/2}}{2} + O(\kappa) \tag{3.5}$$

for the decay rate.

https://doi.org/10.1017/S0022112006003661 Published online by Cambridge University Press

3.2. *WKB analysis*

We introduce the WKB solution

$$\theta(x) = \left(\phi^{(0)}(x) + \kappa^{1/2}\phi^{(1)}(x) + \cdots\right) \mathrm{e}^{f(x)/\kappa^{1/2}}, \tag{3.6}$$

with $\lambda = \lambda^{(0)} + \kappa^{1/2}\lambda^{(1)} + \cdots$, into (3.1) and find at leading order that

$$f(x) = -\frac{wx}{2} \pm \int_0^x (\nu + \mathrm{i}\sin x')^{1/2}\,\mathrm{d}x', \quad \text{with } \nu = \frac{w^2}{4} - \lambda^{(0)}. \tag{3.7}$$

An eigensolution is found if ν can be chosen to ensure that $f(2\pi) = f(0)$. Since the $-$ sign in (3.7) yields a decreasing $\mathrm{Re}\, f(x)$, we focus on the $+$ sign and obtain the condition

$$\int_0^{2\pi} (\nu + \mathrm{i}\sin x)^{1/2}\,\mathrm{d}x = \pi w + 2ni\pi\kappa^{1/2}, \quad n = 0, \pm 1, \pm 2, \cdots. \tag{3.8}$$

In fact, we can take $n = 0$ since other values $n = O(1)$ correspond to an $O(\kappa^{1/2})$ change in λ that can be absorbed in $\lambda^{(1)}$. For $\nu > 0$, (3.8) with $n = 0$ can be satisfied by taking the principal branch of the positive square root. Thus, to leading order, we find the eigenvalue

$$\lambda^{(0)} = \frac{w^2}{4} - \nu_0(w), \tag{3.9}$$

where $\nu_0(w)$ is defined by its inverse $w_0(\nu)$, the elliptic integral

$$w_0(\nu) = \frac{1}{\pi}\int_0^{2\pi} (\nu + \mathrm{i}\sin x)^{1/2}\,\mathrm{d}x \tag{3.10}$$

$$= \frac{4\Gamma\left(\frac{3}{4}\right)^2}{\pi^{3/2}} F\left(-\tfrac{1}{4}, -\tfrac{1}{4}, \tfrac{1}{2}; -\nu^2\right) + \frac{\pi^{1/2}\nu}{\Gamma\left(\frac{3}{4}\right)^2} F\left(\tfrac{1}{4}, \tfrac{1}{4}, \tfrac{3}{2}; -\nu^2\right). \tag{3.11}$$

The second line, giving the integral in terms of hypergeometric functions, is useful in what follows.† It is easy to check from (3.10) that for large w, $\nu_0(w) = w^2/4 - 1/(2w^2) + O(w^{-3})$, so that (3.9) can be identified as the continuation of (3.3) for $w \gg 1$.

At $O(\kappa^{1/2})$, we obtain an equation for $\phi^{(0)}$ with solution

$$\phi^{(0)}(x) = \frac{1}{(f' + w/2)^{1/2}} \exp\left[-\frac{\lambda^{(1)}}{2}\int_0^x \frac{\mathrm{d}x'}{(f'(x') + w/2)}\right].$$

Imposing periodicity gives the purely imaginary corrections $\lambda^{(1)} = nib$, where $n = 0, \pm 1, \pm 2, \cdots$ and b is an easily computed constant. It is only at the next order that the real part of λ depends on n: the $n = 0$ branch is the relevant one for the long-time decay problem, since the corresponding $\mathrm{Re}\,\lambda$ is the largest by an $O(\kappa)$ amount.

So far, we have derived the approximation (3.9) under the assumption that $\nu > 0$. As w decreases from large values, however, $\nu_0(w)$ decreases from a positive value to attain 0 for

$$w = w_* := \frac{4\Gamma\left(\frac{3}{4}\right)^2}{\pi^{3/2}} = 1.0787\cdots \quad \text{with} \quad \lambda^{(0)} = \lambda_* := \frac{w_*^2}{4} = 0.2909\cdots. \tag{3.12}$$

† We thank A. B. Olde Daalhuis for the derivation of this expression.

https://doi.org/10.1017/S0022112006003661 Published online by Cambridge University Press

For $\nu < 0$, we continue to use (3.9), interpreting the integral in (3.10) as the analytic continuation of this integral for $\nu > 0$. This continuation, which involves contributions along branch cuts for $\mathrm{Re}\, x = 0, \pi, 2\pi$, is precisely given by (3.11). Note that obtaining the form of the eigenfuction near $x = 0, \pi, 2\pi$ would require the use of matched asymptotics, since (3.7) breaks down for $\nu < 0$ when the principal branch of the square root is used. We avoid this computation here and rely on the analytic dependence of eigenvalues on parameters (e.g. Kato 1976).

Thus, our WKB analysis gives the approximation

$$\mathrm{Re}\,\lambda = \frac{w^2}{4} - \nu_0(w) + O(\kappa). \tag{3.13}$$

3.3. *Summary*

Our asymptotic analysis provides the two possible approximations (3.5) and (3.13) for the decay rate in the regime (3.4), corresponding to two different eigenvalue branches. It is easy to verify that the two approximations intersect for

$$w = w_* - \kappa^{1/2} s_* + O(\kappa), \tag{3.14}$$

where w_* is given in (3.12) and $s_* = \pi^{1/2}/(2\Gamma(\frac{3}{4})^2) = 0.5901\cdots$. For w smaller (respectively larger) than (3.14), (3.5) (respectively (3.13)) gives the smaller, i.e. relevant, decay rate. That this is non-zero in the limit $\kappa \to 0$ shows that fast mixing can be achieved in a shear flow by a suitable choice of the translation speed. This choice takes $w = O(1)$, i.e. $u = O(\kappa^{1/2})$, to achieve a distinguished limit in the eigenvalue problem (3.1) which leads to eigenfunctions with $O(\kappa^{1/2})$ spatial scales as is required for an $O(1)$ decay rate. Physically, this corresponds to a balance between the two opposite effects that the translation of the sinusoidal flow can have on the scalar damping: an enhancement caused by the continuous shift of the shearless regions of the flow, and an inhibition caused by the periodic reversal of the shear. The largest possible decay rate is obtained by taking w as in (3.14) and is given by

$$\mathrm{Re}\,\lambda = \frac{w_*^2}{4} + \kappa^{1/2}\frac{1 - s_*}{2} + O(\kappa) = 0.2909\cdots + 0.2049\cdots\kappa^{1/2} + O(\kappa). \tag{3.15}$$

The conclusion just drawn presumes that there are no eigenvalue branches with real parts smaller than (3.5) or (3.13). Since this is difficult to establish by asymptotic means only, we rely on numerical solutions of the eigenvalue problem (3.1) to confirm that this is the case and verify the predictions (3.5)–(3.15).

3.4. *Numerical results*

Our numerical procedure is based on a truncated Fourier expansion of θ which transforms (3.1) into a matrix eigenvalue problem, solved by a standard procedure. A truncation retaining 200 to 300 Fourier modes proves sufficient to achieve convergent results for $10^{-3} \leqslant \kappa \leqslant 1$. As we discuss below, the results for significantly smaller κ are crucially affected by round-off errors.

The results are summarized in figure 1. Panel (*a*) shows the real part of the first few eigenvalues (ordered according to their real parts) for $\kappa = 10^{-2}$ as a function of the translation speed u. The comparison with the asymptotic formulae (3.5) and (3.13) confirms that these provide an excellent approximation to the eigenvalue with the smallest real part. Panel (*b*) shows this particular eigenvalue only, but for three values of κ and as a function of the scaled speed w. The eigenvalues collapse to the κ-independent approximation (3.13) to the right of the branch intersection; to the left of this intersection, they match well the approximation (3.5) which gives curves

https://doi.org/10.1017/S0022112006003661 Published online by Cambridge University Press

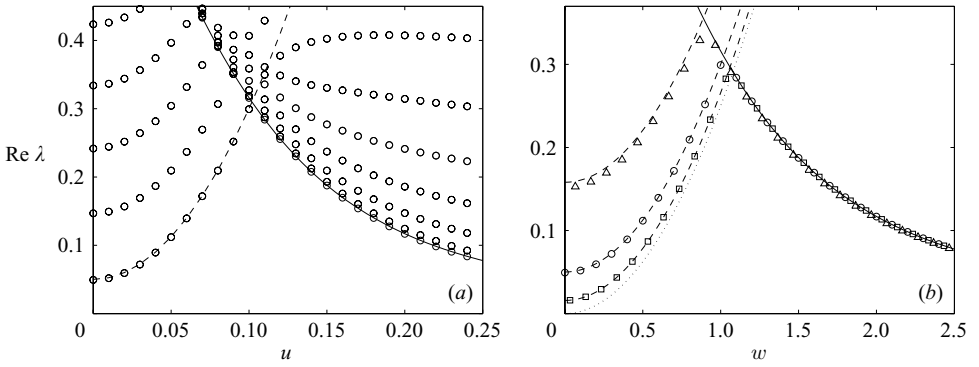


FIGURE 1. Real part of the eigenvalues of the advection–diffusion operator in (3.1) as a function of the translation speed u. (a) Numerical results for $\kappa = 10^{-2}$ ($\circ$) are compared with the two asymptotic estimates (3.5) (dashed line) and (3.13) (solid line) for the eigenvalue with the smallest real part. (b) Numerical estimates of the eigenvalue with smallest real part for $\kappa = 10^{-1}$ ($\triangle$), 10^{-2} ($\circ$) and 10^{-3} ($\square$) are plotted against $w = u/\kappa^{1/2}$. The asymptotic estimates (3.5) (dashed lines) and (3.13) (solid lines) are also shown, with the dotted line indicating the limit of (3.5) as $\kappa \to 0$.

separated by a constant $O(\kappa^{1/2})$ term. (The limit of (3.5) for $\kappa \to 0$, that is the curve $w^2/4$, is indicated by the dotted line.) Figure 1(b) demonstrates the high accuracy of the asymptotic approximations (3.5) and (3.13). In fact, it is likely that the error made for $\mathrm{Re}\,\lambda$ is much smaller than the $O(\kappa)$ our computations suggest.

Our analysis of the eigenvalue problem (3.1) allows us to conclude that a suitable choice of u ensures that the passive-scalar concentration decays exponentially with a decay rate that is independent of κ as $\kappa \to 0$. This exponential decay appears in the long-time limit only, and it is therefore important to estimate the time taken for this limit to be reached. Here, of course, the shear flow (2.1) compares unfavourably with exponentially stretching flows: whilst for the latter the exponential behaviour sets in after a time that scales like $\log(1/\kappa)$, for our shear flows a much longer, $O(\kappa^{-1/2})$, scaling is necessary. This is because the stretching is only linear in time, and the spatial scales need to be reduced to $O(\kappa^{1/2})$ values for the $O(1)$ decay rate to be established.

To confirm this, we present the results of numerical simulations of the advection–diffusion equation (2.3). Figure 2(a) shows the evolution of the L_2 norm $||\hat{C}||(t)$ of the concentration in three simulations with $\kappa = 10^{-3}$, 10^{-2} and 10^{-1}, respectively. The corresponding values of u have been chosen to maximize $\mathrm{Re}\,\lambda$ according to the asymptotic formulae (3.5) and (3.13). As a result, the decay rate is nearly independent of κ, and $||\hat{C}||$ decays at almost the same rate, approximated well by λ_*, in the three simulations. The exponential phase of the decay is seen to occur after a phase of much slower decay which lasts for a time consistent with the expected $\kappa^{1/2}$ scaling. The structure of the decaying scalar after a long time, here $t = 300$, is shown in figure 2(b). The pattern is that predicted by the eigenfunction analysis, with a time-independent profile for $|\hat{C}|/||\hat{C}||$ and a phase propagation observed in $\mathrm{Re}\,\hat{C}$ and $\mathrm{Im}\,\hat{C}$.

The numerical results presented so far have been limited to only moderately small diffusivities $\kappa \geqslant 10^{-3}$. This is because we found that neither the eigenvalue problem nor the time-evolution problem could be solved reliably for smaller diffusivities. To illustrate this, figure 3(a) shows results of the numerical computation of $\mathrm{Re}\,\lambda$ using

https://doi.org/10.1017/S0022112006003661 Published online by Cambridge University Press

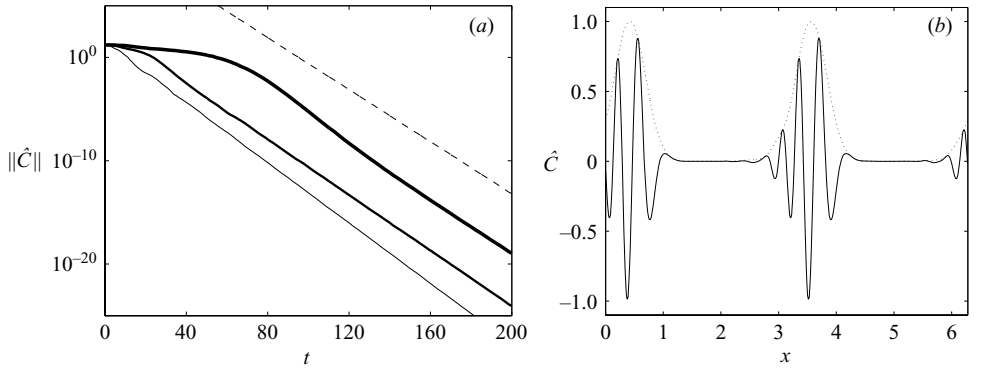


FIGURE 2. (*a*) Evolution of the L_2 norm $||\hat{C}||$ of the concentration in simulations of the advection–diffusion equation (2.3) with $\kappa = 10^{-3}$, 10^{-2} and 10^{-1} (solid lines with decreasing thickness) in lin–log coordinates. The exponential decay expected in the long-time limit for $\kappa \to 0$ is also shown (dashed line). (*b*) Profiles of $\mathrm{Re}\,\hat{C}(x)$ (solid line) and $|\hat{C}(x)|$ (dotted line) normalized by $||\hat{C}||$ obtained for $\kappa = 10^{-3}$ at $t = 300$.

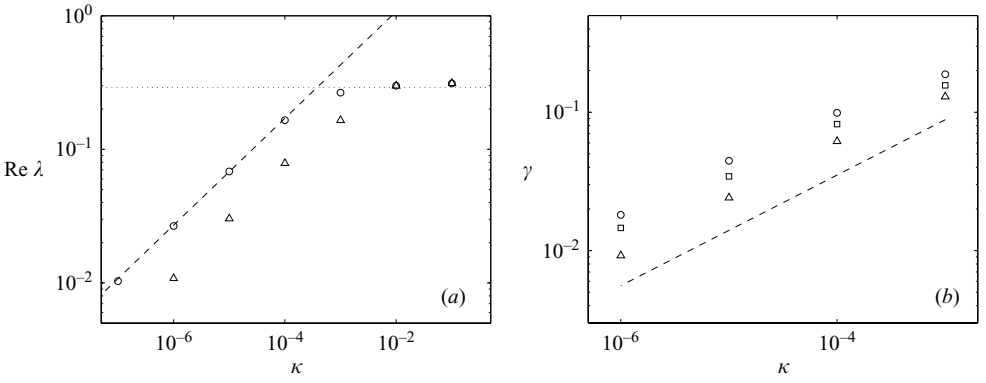


FIGURE 3. (*a*) Real part of the smallest eigenvalue of (3.1) obtained numerically for $w = u/\kappa^{1/2} = 1$ as a function of the diffusivity κ. Results of double-precision (○) and single-precision (△) computations are shown, together with the asymptotic result $\mathrm{Re}\,\lambda \sim \lambda_*$ (dotted line). The departure from this asymptotic behaviour for $\kappa \lesssim 10^{-3}$ can be attributed to round-off errors; this leads to the decay of $\mathrm{Re}\,\lambda$ according to the $\kappa^{2/5}$ power law indicated by a dashed line. (*b*) Decay rate γ as a function of κ in simulations with external noise with amplitude $A = 10^{-3}$ (△), 10^{-2} (□) and 10^{-1} (○). A $\kappa^{2/5}$ dependence similar to that in (*a*) is indicated by the dashed line.

double- and single-precision arithmetic. These show that the prediction that $\mathrm{Re}\,\lambda$ tends to a non-zero value as $\kappa \to 0$ is not robust: the noise introduced by round-off errors leads to $\mathrm{Re}\,\lambda = o(1)$. More specifically, $\mathrm{Re}\,\lambda \to 0$ with what appears to be a $\kappa^{2/5}$ power law. The prefactor of the power law changes between double- and single-precision computations (effectively a change in the noise intensity), but the behaviour is robust to changes in other details of the numerical implementation such as truncation and algorithm choice. Note that the eigenvalues found numerically are also consistent with the numerical solutions of the time-evolution problem. In this case, the evolution is not exponential, but a decay rate can be defined, say as $\gamma = t^{-1}\log[||C||(t)/||C||(0)]$, which nearly coincides with the eigenvalue.

https://doi.org/10.1017/S0022112006003661 Published online by Cambridge University Press

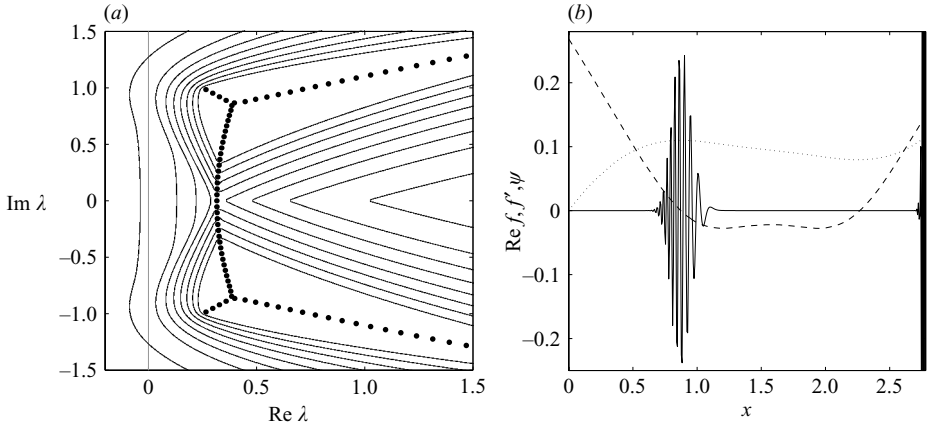


FIGURE 4. (*a*) Spectrum (symbols) and ε-pseudospectra of the advection–diffusion operator in (3.1) with $\kappa = 10^{-3}$ and $w = u/\kappa^{1/2} = 1$. The contours mark the boundary of the ε-pseudospectra with $\varepsilon = 10^{-1}, 10^{-2}, \cdots, 10^{-8}$. (*b*) Construction of a pseudomode. The real parts of $f(x)$ (dotted line), defined in (3.7), of its derivative (dashed line), and of the rough approximation $\psi = \exp[f(x)/\kappa^{1/2}]$ to the WKB solution obtained for $w = 1$ and $\lambda = 0.0267 + \mathrm{i}\,0.930$ are shown in an interval of x surrounding the local maximum $x_* = 0.89$ of $\mathrm{Re}\, f(x)$.

We argue that the behaviour of $\mathrm{Re}\,\lambda$ and γ in the presence of round-off error is relevant physically, since the noise induced is not fundamentally different from other, physical, noises such as fluctuations in the advecting velocity field or in the concentration field. This is confirmed by figure 3(*b*) which shows the decay rate γ estimated from numerical simulations of the time-evolution problem (2.3) perturbed by the small multiplicative noise $A\eta(x,t)\hat{C}(x,t)$, where A is an amplitude, ranging from 10^{-3} to 10^{-1}, and $\eta(x,t)$ is a space–time white noise. The $\kappa^{2/5}$-dependence of γ observed with round-off error is recovered, with a prefactor that decreases as the noise level increases. In view of its relevance, both physical and numerical, it is worthwhile examining the cause of this $\kappa^{2/5}$ power law. In the next section, we attribute it to the existence of pseudomodes for the operator in (3.1), that is, approximate solutions of (3.1) with exponentially small errors.

4. Pseudomodes

As discussed by Reddy & Trefethen (1994), advection–diffusion operators such as that in (3.1) have spectra that are highly sensitive to perturbations in the large-Péclet-number limit $\kappa \to 0$. This can be quantified by noting that the ε-pseudospectrum (Trefethen 1997; Trefethen & Embree 2005) can be an $O(1)$ distance away from the spectrum for ε exponentially small in κ. This is illustrated by figure 4(*a*) which shows the spectrum and pseudospectra of (3.1) for $\kappa = 10^{-3}$ and $w = 1$ computed using the EigTool package (Wright 2002). Significant distances between the spectrum and the boundary of the pseudospectra for small ε are observed, notably for small $\mathrm{Re}\,\lambda$ in the region $\mathrm{Im}\,\lambda \approx \pm 1$. The nature of the pseudospectra can be explained by the existence of exponentially accurate pseudomodes (Dencker, Sjöstrand & Zworski 2004; Trefethen 2005). In our context, existence of pseudomodes with $\mathrm{Re}\,\lambda < \lambda_*$ implies that the passive-scalar decay can be significantly slower than $\exp(-\lambda_* t)$ if the advection–diffusion system is perturbed, for instance by external noise.

https://doi.org/10.1017/S0022112006003661 Published online by Cambridge University Press

Pseudomodes are easily constructed from the WKB analysis in § 3.2. Indeed, if $\mathrm{Re}\, f(x)$ has a local maximum $x_* > 0$ for a given λ, that is $\mathrm{Re}\, f'(x_*) = 0$, $\mathrm{Re}\, f''(x_*) < 0$, then a pseudomode localized near x_* can be built by taking the WKB solution in an $O(1)$-neighbourhood of x_* and joining it smoothly to 0 outside this neighbourhood so that the periodic boundary conditions are satisfied. Since the switch from one solution of (3.1) (the WKB solution) to another one ($\equiv 0$) is made where the former solution is exponentially small, the result is exponentially close to an eigensolution, even though λ is distant from the spectrum. This type of argument can be made rigorous (Dencker *et al.* 2004; Trefethen 2005), but the heuristic justification just given is sufficient for our purpose.

The construction of a pseudomode is illustrated in figure 4(*b*). This shows $\mathrm{Re}\, f(x)$ and $\mathrm{Re}\, f'(x)$ for $w = 1$ and $\lambda = 0.0267 + \mathrm{i}\,0.930$ (the smallest eigenvalue found numerically for $\kappa = 10^{-6}$). In the range of $0 < x < 2.6$, $f(x)$ has a maximum at $x_* = 0.89$, and a local minimum at $\pi - x_* = 2.25$. Correspondingly, the WKB solution has the form of a wavepacket localized near x_*. For $x > 2.6$, $\mathrm{Re}\, f(x)$ increases well above $\mathrm{Re}\, f(x_*)$, and the WKB solution grows widely, as the extreme right of the figure suggests. This, however, does not affect the construction of the pseudomode, since the WKB solution is replaced by 0 in that region. Note that an optimum pseudomode, in the sense that it approximates a solution of (3.1) for fixed λ with minimum error, is constructed by switching from the WKB solution to 0 in a neighbourhood of $\pi - x_*$, where $\mathrm{Re}\, f(x)$ is minimum.

Among all the possible pseudomodes, it is intuitive that the ones with smallest $\mathrm{Re}\,\lambda$ are the most important for the dynamics since they decay most slowly. However, for fixed κ, there is a limitation in how small $\mathrm{Re}\,\lambda$ can be. This limitation, which we now examine, is key to the $\kappa^{2/5}$ power law observed in the presence of noise. We first note that the small values of $\mathrm{Re}\,\lambda$ found in our numerical solution of the eigenvalue problem for $w = 1$ correspond to $\mathrm{Im}\,\lambda$ close to ± 1 (see figure 4), with $x_* \approx \pi/2$ or $3\pi/2$. Focusing on $\mathrm{Im}\,\lambda > 0$, and seeking a distinguished scaling, we let

$$\lambda = \mathrm{i}(1 + \epsilon^2 \lambda_i) + \epsilon^4 \lambda_r \quad \text{and} \quad x = \pi/2 + \epsilon\xi, \tag{4.1}$$

where ϵ is a small parameter, and λ_i, λ_r and ξ are $O(1)$ constants. Introducing into the expression of $f'(x)$ and solving for x_* gives the approximation

$$x_* = \pi/2 + \epsilon\xi_*, \quad \text{with } \xi_* = -2^{1/2}\left(w\lambda_r^{1/2} - \lambda_i\right)^{1/2}.$$

(There may be two additional zeros between x_* and $\pi - x_*$, but these do not change the structure of the WKB solution.) If, as argued above, a pseudomode is constructed optimally by replacing the WKB solution by zero where this solution is the smallest, that is at $\pi - x_*$, the error made in the eigenvalue problem is roughly $\exp(-\alpha)$, where

$$\alpha = \frac{f(x_*) - f(\pi - x_*)}{\kappa^{1/2}}$$

can be termed 'attenuation factor'. With the scaling in (4.1), this factor is approximately

$$\alpha \sim \frac{8\epsilon^5\left(w\lambda_r^{1/2} - \lambda_i\right)^{3/2}\left(3w\lambda_r^{1/2} + 2\lambda_i\right)^{1/2}}{15w^3\kappa^{1/2}}.$$

Only pseudomodes with a sufficiently small error are susceptible to being excited by small external noise: this requires that α be sufficiently large and hence that $\epsilon \geqslant O(\kappa^{1/10})$. Returning to (4.1), we therefore obtain the scaling $\mathrm{Re}\,\lambda = O(\kappa^{2/5})$ consistent with the numerical results of § 3.4. The additional scalings $\mathrm{Im}\,\lambda = \mathrm{i} + O(\kappa^{1/5})$

https://doi.org/10.1017/S0022112006003661 Published online by Cambridge University Press

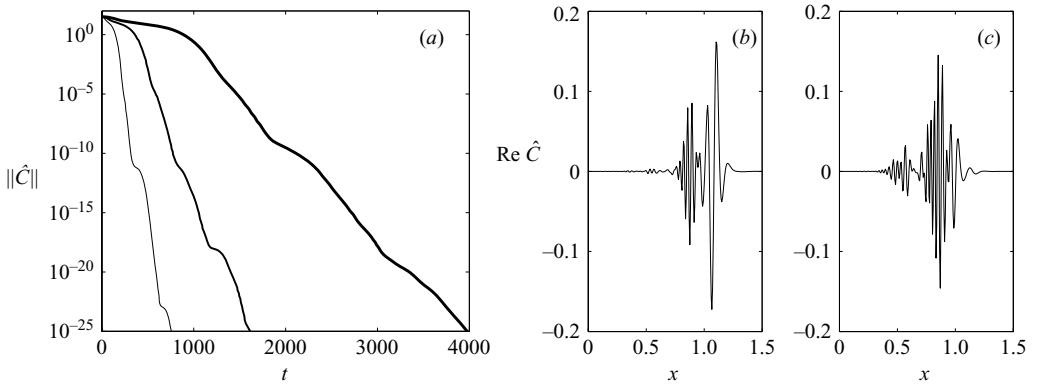


FIGURE 5. Evolution of the concentration in the presence of a small noise. (a) The evolution of the L_2 norm $||\hat{C}||$ of the concentration for $\kappa = 10^{-6}$, 10^{-5} and 10^{-4} (solid lines with decreasing thickness). (b, c) The concentration profile for $\kappa = 10^{-6}$ at $t = 2150$ and $t = 4000$, respectively.

and $x_* - \pi/2 = O(\kappa^{1/10})$ are also consistent with the eigenvalues and eigenfunctions found numerically (not shown) when the round-off error plays a major role.

Further insight in the role of the pseudomodes can be gained from figure 5. Figure 5(a) shows the evolution of the concentration in simulations with multiplicative noise with amplitude $A = 10^{-3}$ and for three values of κ. The evolution is akin to a succession of transient events caused by the noise. The structure of $\hat{C}$ is highly transient, but its gross features stay similar throughout the simulation, with two highly oscillatory peaks shifted by π. This is illustrated by figures 5(b) and 5(c) showing $\mathrm{Re}\,\hat{C}$ obtained for $\kappa = 10^{-6}$ at two different times. These plots focus on the range $0 \leqslant x \leqslant 1.5$, so a single peak appears in each. Whilst one cannot associate a single pseudomode to each peak, as their form is continuously evolving as a result of the noise, comparison with the pseudomodes with small $\mathrm{Re}\,\lambda$ and $\mathrm{Im}\,\lambda$ near ± 1 strongly suggests that these play a crucial role in the dynamics.

5. Discussion

The main conclusion of the paper is as follows. In the translating shear flow (2.1) or equivalently the steady two-dimensional flow $(-u, \alpha \sin x)$, the decay rate of a passive scalar can be arranged to be $O(1)$ in the small-diffusivity limit $\kappa \to 0$ by a suitable choice of u. Specifically, taking $u = O(\kappa^{1/2})$ gives a decay rate

$$\mathrm{Re}\,\lambda \sim f(w), \tag{5.1}$$

where $f(w)$ is an $O(1)$ function given either by the first term in (3.5) or by (3.13) depending on whether $w = u/\kappa^{1/2}$ is smaller or larger than $w_* = 1.0787\cdots$.

This conclusion has been reached by considering a single Fourier mode $l \neq 0$ in the y-direction, but it is easily verified that it implies that a suitable choice of u leads to an $O(1)$ decay rate of all the non-zero Fourier modes, and therefore to the fast decay of any concentration distribution with zero y-average. To see this, we return to the unscaled variables λ, u and κ used in (2.1)–(2.2), and rewrite (5.1) as

$$\frac{L}{\alpha}\mathrm{Re}\,\lambda \sim nf\left(n^{-1/2}w\right), \quad \text{where } w = \frac{L^{1/2}u}{(\alpha\kappa)^{1/2}}$$

https://doi.org/10.1017/S0022112006003661 Published online by Cambridge University Press

and $n = 1, 2, \cdots$ characterizes the Fourier mode. Choosing u such that $w = w_*$ means that $f(\cdot)$ is defined by the first term in (3.5) and hence that

$$\frac{L}{\alpha}\mathrm{Re}\,\lambda \sim \frac{w_*^2}{4} \quad \text{for } n = 1, 2, \cdots$$

as $\kappa \to 0$. Thus all the non-zero Fourier modes have asymptotically the same decay rate. (In fact, the $O(\kappa^{1/2})$ correction in (3.5) adds a term proportional to $n\kappa^{1/2}$ to the decay rate, so that the higher modes $n > 1$ experience faster decay.)

Our results also indicate that the non-zero limit of the decay rate as $\kappa \to 0$ is fragile, as might be expected from the non-normality of the governing eigenvalue problem. This is quantified by showing that the decay rate decreases to zero like $\kappa^{2/5}$ in the presence of a small noise, and is explained in terms of pseudomodes. We note that the pseudomodal behaviour may be relevant to the situation recently examined by Vanneste (2006) where the shear flow translates randomly in time rather than steadily.

The authors thank S. J. Cowley and L. N. Trefethen for useful suggestions. J. V. is funded by a NERC Advanced Research Fellowship.

REFERENCES

Antonsen, T. M., Fan, Z., Ott, E. & Garcia-Lopez, E. 1996 The role of chaotic orbits in the determination of power spectra of passive scalar. *Phys. Fluids* **8**, 3094–3104.

Bajer, K., Bassom, A. P. & Gilbert, A. D. 2001 Accelerated diffusion in the centre of a vortex. *J. Fluid Mech.* **437**, 395–411.

Childress, S. & Soward, A. M. 1990 Large magnetic Reynolds number dynamo action in spatially periodic flow with mean motion. *Phil. Trans. R. Soc. Lond.* A **331**, 649–733.

Dencker, N., Sjöstrand, J. & Zworski, M. 2004 Pseudospectra of semiclassical (pseudo-) differential operators. *Commun. Pure Appl. Maths* **57**, 384–415.

Giona, M., Cerbelli, S. & Vitacolonna, V. 2004 Universality and imaginary potentials in advection–diffusion in closed flows. *J. Fluid Mech.* **513**, 221–237.

Gleeson, J. P., Roche, O. M., West, J. & Gelb, A. 2004 Modelling angular micromixers. *SIAM J. Appl. Maths* **64**, 1294–1310.

Haynes, P. H. & Vanneste, J. 2005 What controls the decay rate of passive scalars in smooth random flows? *Phys. Fluids* **17**, 097103.

Kato, T. 1976 *Perturbation Theory for Linear Operators*, 2nd edn. Springer.

Majda, A. J. & McLaughlin, R. M. 1993 The effect of mean flows on enhanced diffusivity and transport by incompressible periodic velocity fields. *Stud. Appl. Maths* **89**, 245–279.

Pierrehumbert, R. T. 1994 Tracer microstructure in the large-eddy dominated regime. *Chaos, Solitons Fractals* **4**, 1091–1110.

Reddy, S. C. & Trefethen, L. N. 1994 Pseudospectra of converction–diffusion operator. *SIAM J. Appl. Maths* **54**, 1634–1649.

Trefethen, L. 1997 Pseudospectra of linear operators. *SIAM Rev.* **39**, 383–406.

Trefethen, L. 2005 Wave packet pseudomodes of variable coefficient differential operators. *Proc. R. Soc. Lond.* A **461**, 3099–3122.

Trefethen, L. N. & Embree, M. 2005 *Spectra and Pseudospectra: The Behaviour of Nonnormal Matrices and Operators*. Princeton University Press.

Tsang, Y.-K., Antonsen, T. M. & Ott, E. 2005 Exponential decay of chaotically advected passive scalars in the zero diffusivity limit. *Phys. Rev.* E **71**, 066313.

Vanneste, J. 2006 Intermittency of passive-scalar decay: strange eigenmodes in random shear flows. *Phys. Fluids* **18**, 087108.

Wiggins, S. & Ottino, J. M. 2004 Foundation of chaotic mixing. *Phil. Trans. R. Soc. Lond.* A **362**, 937–970.

Wright, T. 2002 *EigTool: a graphical tool for nonsymmetric eigenproblems*. Available at: http://web.comlab.ox.ac.uk/projects/pseudospectra/eigtool/.

https://doi.org/10.1017/S0022112006003661 Published online by Cambridge University Press